Journal of Chromatography, 554 (1991) 155–173
Elsevier Science Publishers B.V., Amsterdam

CHROMSYMP. 2339

Use of methyl oxime derivatives to enhance structural information in thermospray high-performance liquid chromatography–mass spectrometry

Analysis of linoleic acid lipoxygenase metabolites in maize embryos

J. ABIÁN
Department of Neurochemistry, Centro de Investigación y Desarrollo, CSIC, Jordi Girona 18–26, 08034 Barcelona (Spain)
M. PAGÈS
Department of Molecular Genetics, Centro de Investigación y Desarrollo, CSIC, Jordi Girona 18–26, 08034 Barcelona (Spain)
and
E. GELPÍ*
Department of Neurochemistry, Centro de Investigación y Desarrollo, CSIC, Jordi Girona 18–26, 08034 Barcelona (Spain)

ABSTRACT

Lipoxygenase derived metabolites of linoleic acid generated by incubation with protein extracts from maize embryos treated with abscisic acid have been analysed by thermospray high-performance liquid chromatography–mass spectrometry (HPLC–TSP-MS). TSP-MS data for various isomeric α- and γ-ketols, ketodiols and trihydroxyacids are reported. The molecular weight and the minimum number of oxygenated functions in the structures can be readily characterized from the TSP spectra obtained in the positive and negative ion modes of acquisition. TSP analysis of the methoximated compounds allows the characterization of ketone or aldehyde groups. Additionally, the methoximated derivatives show abundant ions derived from concomitant losses of methanol and the breakdown of the C–C bond α to the methoxime. These ions are the base peaks in the TSP spectra of compounds bearing an α-ketol moiety in their structures. The TSP data and fragment assignments are in agreement with the structures previously elucidated by gas chromatography (GC)–MS techniques. Furthermore, the characteristic fragmentation pattern of the methoxime derivatives allows the characterization of a pair of positional isomer α-ketols not detected previously by GC–MS. Some of these metabolites have not been described before in maize.

INTRODUCTION

Lipoxygenase (LOX) activity was initially discovered in the plant kingdom where the most common substrates are linoleic (LA) and linolenic acid. In general,

0021-9673/91/$03.50

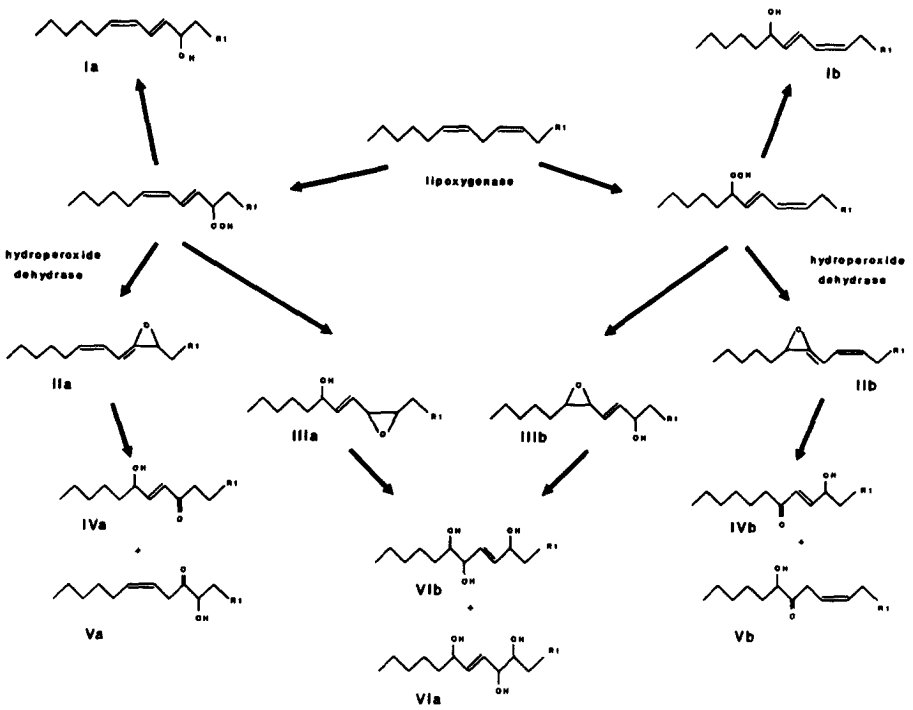

Fig. 1. LOX metabolic pathways of LA leading to linear chain C_{18} acids. R1 is $(CH_2)_6COOH$.

LOX in plants catalyses the addition of oxygen to positions *n*-6 or *n*-10 of the fatty acid, giving rise to conjugated hydroperoxyoctadecadienes (HPODEs) such as the 9- or 13-HPODEs. These HPODEs can either be reduced to their corresponding hydroxy acids (9- or 13-HODEs) or they can generate α- and γ-ketols, various short chain aldehydes and oxo acids and a group of compounds structurally similar to prostaglandins, with 12-oxo-phytodienoic acid as the parent compound [1]. Some of the LOX derived metabolites of LA detected to date in various plant sources are illustrated in Fig. 1. The physiological role of these compounds is for the most part still to be determined, although they seem to be implicated in growth and development, senescence and responses to physical or pest derived injuries [1,2].

Work has recently been completed on the identification of LOX metabolites of LA in maize embryos using gas chromatography–mass spectrometry (GC–MS) and on the effect of abscisic acid (ABA) on this metabolism during embriogenesis [3]. ABA is a plant hormone that regulates growth during seed maturation [4]. In the course of this work the role of thermospray high-performance liquid chromatography–mass spectrometry (HPLC–TSP-MS) in this type of application was evaluated. This paper shows how TSP can provide not only molecular but also structural information leading to the identification of individual metabolites, verified by GC–MS. Along these lines we illustrate the identification of new metabolites based only on the analysis of data from TSP-MS; to our knowledge this is a unique example of new compound identification by TSP-MS.

MATERIALS AND METHODS

Reagents

LA was obtained from Merck (Darmstadt, Germany) and [1-^{14}C] LA (59 mCi/mmol) from New England Nuclear (Du Pont de Nemours, Dreieich, Germany).

The scintillation liquid, Unisolve 1, was from Koch-Light (Colnbrook, UK). The derivatization reagents used were 1-methyl-3-nitro-1-nitrosoguanidine (Aldrich-Chemie, Steinheim, Germany) and methoxyamine hydrochloride (Eastman Kodak, Rochester, NY, USA).

The water used in the HPLC eluents was of Milli-Q grade (Waters Assoc., Milford, MA, USA) and was passed through a 0.45-μm filter. The other reagents and solvents were of analytical or spectroscopic grade.

Plant material

Isolated embryos of Zea maize L inbred line W-64 at different stages of development (from 15 days after pollination to dry embryos) were used. Incubation of embryos in the presence of ABA was performed by culturing the isolated embryos for 7 days in basal medium with 10 μM ABA, as described previously [5].

Enzyme extracts

Extracts from control and ABA incubated embryos were prepared by grinding the fresh material in a mortar with liquid nitrogen [6]. A 100–200-mg mass of powder was immediately sonicated in 1 ml of 0.05 *M* phosphate buffer (pH 7) (2% sodium metabisulphite). The samples were centrifuged and the supernatants were used for the incubation with LA.

Oxidation products of linoleic acid

A 100-μg mass of LA and 0.5 μCi of [1-^{14}C] LA were added to 4 ml of 0.05 *M* phosphate buffer (pH 6) with 500–800 μl of the enzyme extract. To avoid the presence of LA autooxidation products, both LA and [1-^{14}C] LA were previously purified and monitored by reversed-phase HPLC. The incubation was carried out at room temperature for 30 min with vigorous shaking and in the presence of air.

Residual hydroperoxides in the media were then reduced by the addition of 500 μl of tin(II) chloride (1 mg/ml in ethanol). After a 30 min reaction time the incubation media were saturated with sodium chloride and extracted at pH 3 with diethyl ether. The ethereal extracts were dried with anhydrous sodium sulphate and evaporated to dryness under a stream of helium. The residue was redisolved in acetonitrile (ACN) and stored at -80°C until analysis.

Liquid chromatography

The HPLC separations were carried out using a reversed-phase 10 μm (30 × 0.4 cm) Spherisorb ODS-2 column (Phase Separations, Queensferry, UK). The mobile phase was water (pH 3.5 with acetic acid) with a gradient of ACN from 30 to 95% in 30 min.

Radioactivity was detected using an on-line LS detector (Ramona, RAYTEST) or by the counting radioactivity of sequential 30 s fractions in a Beckman LS counter detector.

Derivatization

Methylation and methoximation were carried out by standard procedures (ethereal diazomethane and methoxyamine hydrochloride in pyridine as reagents, respectively) as described previously [7]. Derivatized fractions were redisolved in methanol and injected directly in the TSP system.

HPLC–TSP-MS

A Hewlett Packard 5988A quadrupole instrument with a Vestal type TSP source and interface was used.

The chromatography was accomplished using a 5 μm (15 × 0.4 cm) Spherisorb ODS-2 reversed-phase column. The mobile phase consisted of mixtures of 0.1 *M* ammonium acetate buffer (AMAC) and 0.05 *M* AMAC in methanol. The specific HPLC–TSP-MS conditions and gradient programmes are given in Tables I–VII.

The amount of LA metabolites injected for each TSP-MS analysis (full scan acquisition) was around 0.1–0.5 μg as measured by the total radioactivity counted in each HPLC fraction and for a theoretical 100% extraction recovery.

Metabolite characterization by GC–MS

Compounds in the major radioactive HPLC fractions were characterized by GC–MS techniques as described elsewhere [3].

RESULTS AND DISCUSSION

Radiochromatography profiles and TSP-MS analysis of selected HPLC fractions

The radiochromatographic profiles from extracts of 15-day-old maize embryos treated or untreated with ABA are shown in Fig. 2.

Under the described incubation conditions only minor amounts of unmetabolized LA could be detected. Various radioactive peaks were observed in these profiles and eight of these were amenable to analysis by MS, their individual abundances varying with ABA treatment and stage of development. All of theses peaks disappeared after the extracts were deactivated by heat at 100°C for 1 min prior to incubation.

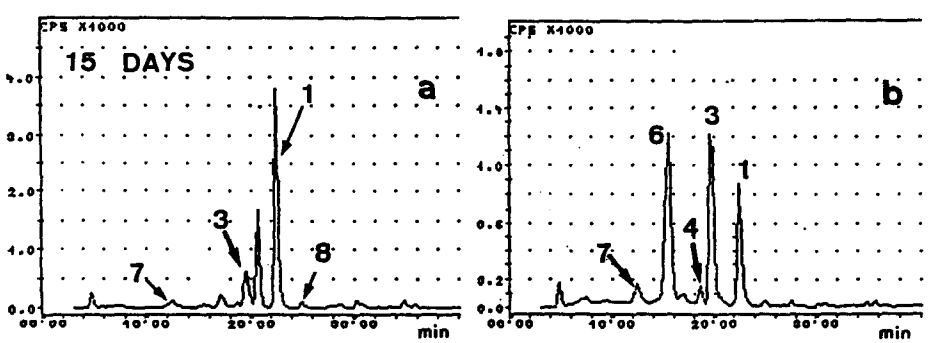

Fig. 2. HPLC radiochromatograms obtained from incubates of [1-14C]LA with maize embryo extracts 15 days after polinization. (a) Control; (b) sample treated with ABA as described under Experimental.

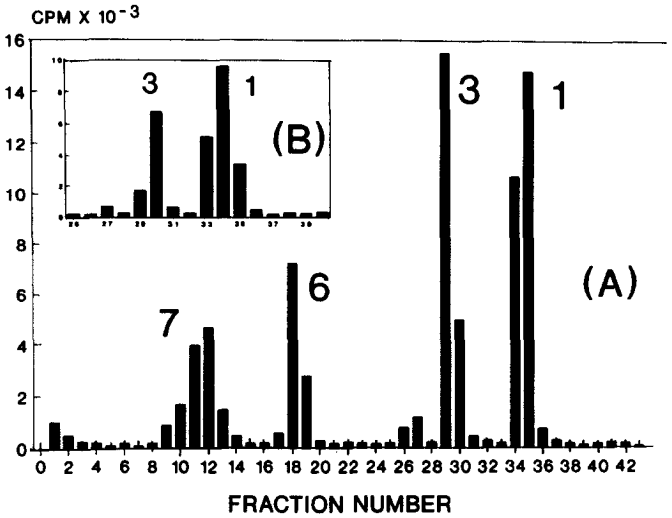

Fig. 3 (A) HPLC reconstructed radiochromatogram with indication of fraction numbers. Peaks 1, 3, 6 and 7 indicating the major radioactive fractions correspond to the same peaks shown in Fig. 2b. Partial profile from a different experiment. Fractions 33–35 in this profile were selected for a more accurate analysis of the composition of peak 1.

The most pronounced change in the profile is that observed in the appearance and high relative abundance of peak 6 when young embryos are exposed to ABA, especially in the earlier stages of development (Fig. 2b). The peak, which can hardly be detected at 15 days without ABA treatment (Fig. 2a), attains a height equivalent to that of peak 3 after ABA treatment. The induction of peak 6 gradually decreases with maturation and disappears in the dry embryos. During normal embryogenesis this

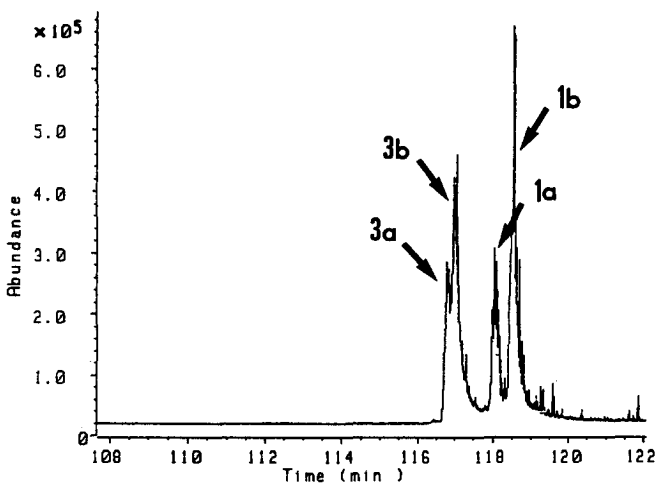

Fig. 4. Reversed-phase TSP-MS chromatogram of a 1:1 mixture of the central fractions obtained from peak 1 (peaks 1a and b) and peak 3 (peaks 3a and b) in Fig. 2.

peak can be detected during the period in which endogenous levels of ABA are at a maximum. Peak 1 also undergoes a significant ABA-induced change, decreasing by approximately four-fold.

The compounds labelled 1, 3, 6 and 7 in the radiochromatograms of Fig. 2 were analysed by HPLC–TSP-MS and the results were confirmed by GC–MS [3]. For this purpose the embryo incubates were fractionated by HPLC and 30 s fractions were individually collected. An example of the reconstructed radiochromatograms for two different extracts is shown in Fig. 3. Fig. 3b corresponds to part of the sample used for a more detailed study of the components in peak 1.

TSP-MS analysis of fractions from peak 1

The eluate fractions corresponding to peak 1 (fractions 33–35 in Fig. 3b) show the presence of two components with identical TSP-MS spectra, indicated as 1a and 1b in Fig. 4. Both can be assigned a molecular weight of 312 in accordance with the data in Table I. In the TSP-MS positive ion mode (Table Ia) the mass of the base peaks corresponds to that of an ammonium adduct and in the negative mode (Table Ib) the base peak corresponds to $[M-H]^-$, whereas abundant M^- ions can also be seen with the filament on. Ions arising from the loss of water are abundant both in the

TABLE I

HPLC–TSP-MS SPECTRA OF COMPOUNDS IN HPLC FRACTIONS CORRESPONDING TO PEAKS 1 AND 3

Positive ions: filament on; negative ions: filament on or off, as indicated. HPLC eluents: A = 0.1 *M* ammonium acetate buffer; B = 0.05 *M* ammonium acetate in methanol. HPLC gradient programme: 60–75% B in 10 min; Flow-rate, 1 ml/min; interface, 96°C; vaporizer exit, 181°C; ion source, 270°C. [ASSIGN] molecular assignment according to observed *m/z* value of ion; AcO = acetate. The corresponding relative abundances of ions are shown under 1a, 1b and 3a + 3b. HPLC–TSP-MS retention times are shown in parentheses in Table Ia.

[ASSIGN]$^+$	*m/z*	1a (12.6)		1b (13.1)		3a + 3b (11.3,11.6)	
(a) *Positive ions*							
$M+NH_4-2H_2O$	294	5		–		2	
$M+H-H_2O$	295	26		12		46	
$M+NH_4-H_2O$	312	8		–		16	
M + H	313	19		14		64	
$M+NH_4$	330	100		100		100	
		1a		1b		3a + 3b	
		On	Off	On	Off	On	Off
(b) *Negative ions*							
$M-H-H_2O$	293	7	8	3	4	11	8
$M-H_2O$	294	8	2	4	1	42	2
M − H	311	100	100	100	100	100	100
M	312	50	14	64	20	42	16
M + Cl	347	12	2	14	2	14	2
M + AcO − H_2O	353	4	5	5	2	7	5
M + AcO	371	3	2	1	4	11	7

positive and in the negative ion mode, indicating the presence of at least one hydroxyl group in the molecule.

TSP–MS analysis of fractions from peak 3

The HPLC eluate fractions corresponding to the retention time of peak 3 (fractions 29–30 in Fig. 3) also show the presence of two components with TSP-MS features identical to those of the components found in peak 1 (Table I). These two compounds are indicated as 3a and 3b in Fig. 4.

The spectra obtained by TSP-MS across the peak band profiles of peak 1a, b and 3a, b (Fig. 4) show differences in the extent of dehydration processes as well as in the ion ratios $[M+H]^+/[M+NH_4]^+$ and $[M-H-H_2O]^-/[M-H_2O]^-$ (see Table I). The apparently higher relative proton affinity of this pair of isomers and the extent of water elimination, which is consistent with an additional oxygenated structural moiety leading to the elimination of water (hydroxyl, ketone or aldehyde function), together with the importance of electron capture ions due to water losses suggest a conjugated system in which conjugation is enhanced by dehydration processes.

TSP-MS analysis of fractions from peak 6

Fractions collected at the retention time of peak 6 (fractions 18–19 in Fig. 3) produce a wide but homogeneous peak on HPLC–TSP-MS analysis. The molecular weight deduced from the spectra obtained by TSP-MS is 328 a.m.u. (Table II). The mass spectrum is characterized by the abundance of signals arising from losses of up to two water molecules.

TSP-MS analysis of fractions from peak 7

The fraction collected across the elution pattern of peak 7 (fractions 10–13 in Fig. 3) also show an homogeneous peak in the HPLC–TSP-MS spectra with a molecular weight at 330 a.m.u. (Table III). The positive ion mode TSP-MS spectrum corresponds to that of a compound with a relatively lower proton affinity and thus more

TABLE II

HPLC–TSP-MS SPECTRA OF COMPOUNDS IN HPLC FRACTIONS CORRESPONDING TO PEAK 6

Eluent: 0.1 *M* AMAC–methanol (0.05 *M* ammonium acetate) (3:7). Flow-rate, 1 ml/min; interface, 104°C; vaporizer exit, 180°C; ion source, 270°C; filament on. RA = Relative abundances of ions. See also Table I.

Positive ions			Negative ions		
$[ASSIGN]^+$	*m/z*	RA	$[ASSIGN]^-$	*m/z*	RA
$M+H-2H_2O$	293	25	$M-H-2H_2O$	291	–
$M+NH_4-2H_2O$	310	17	$M-2H_2O$	292	12
$M+H-H_2O$	311	66	$M-H-H_2O$	309	13
$M+NH_4-H_2O$	328	76	$M-H_2O$	310	100
$M+H$	329	42	$M-H$	327	21
$M+NH_4$	346	100	M	328	14
			M + AcO	369	1
			M + AcOH	370	3

TABLE III

HPLC–TSP-MS SPECTRA OF COMPOUNDS IN HPLC FRACTIONS CORRESPONDING TO PEAK 7

HPLC eluent: 30% 0.1 *M* ammonium acetate buffer–70% 0.05 *M* ammonium acetate in methanol. Flow-rate, 1 ml/min; interface, 104°C; vaporizer exit, 180°C; ion source, 270°C; filament on. RA = Relative abundances of ions. See also Table I.

Positive ions			Negative ions		
$[ASSIGN]^+$	*m/z*	RA	$[ASSIGN]^-$	*m/z*	RA
$M+H-3H_2O$	277	7	$M-H-3H_2O$	275	3
$M+NH_4-3H_2O$	294	6	$M-3H_2O$	276	4
$M+H-2H_2O$	295	100	$M-H-2H_2O$	293	33
$M+NH_4-2H_2O$	312	50	$M-2H_2O$	294	96
$M+H-H_2O$	313	19	$M-H-H_2O$	311	12
$M+NH_4-H_2O$	330	17	$M-H_2O$	312	17
$M+H$	331	5	$M-H$	329	100
$M+NH_4$	348	67	M	330	19
			M + AcO	359	–
			M + AcOH	360	–

abundant $(M+NH_4]^+$ and $[M+NH_4-H_2O]^+$ ions. In this instance, ions generated by the loss of two water molecules can be readily observed and the base peak at $[M+H-2H_2O]^+$ is twice as high as the corresponding ammonium adduct. In the negative ion mode the base peak corresponds to the $[M-H]^-$ ion and the loss of two water molecules can also be observed. Electron capture processes are also apparent in the more dehydrated forms.

Methoxime derivatives of selected HPLC fractions

According to the TSP-MS data the components of HPLC peaks 1, 3, 6 and 7 (see Fig. 2) can be tentatively characterized as di- or trioxygenated derivatives of LA with various unsaturation centres as a result of the presence of double bonds, cyclic structures, epoxides and ketone or aldehyde groups. The last two groups can be readily determined by previous methoximation of the samples. Methoxime (MO) derivatives show molecular weight peaks at 29 a.m.u. greater than those of the original ketone or aldehyde groups present in the analyte molecule. It has recently been shown that the TSP spectrum of methoximated thromboxane B_2, a compound bearing an aldehyde group, is characterized by important signals due to losses of methanol [8]. In contrast, the methoximes of compounds with keto groups positioned in linear chains or cyclic structures, such as in prostaglandin (PG) 6-keto $PGF_{1\alpha}$ or prostaglandins PGE_2 and PGD_2, predominantly show ions derived from the hydrolysis or ammoniolysis of the methoxime group [7]. Low abundance ions derived from methanol losses in these prostaglandins seem to be related to fragmentation of the C–C bonds α to the methoxime group, giving rise to a nitrile structure. Accordingly, the TSP-MS spectra of methoximated 6-keto $PGF_{1\alpha}$ show ions derived from the combined losses of methanol and the C1–C5 carboxylic linear chain [9]. Methoxime formation is therefore able to differentiate between aldehydes and ketones and could therefore give useful structural information.

Methoxime derivatives of fractions from peak 1

After methoxime formation, the TSP-MS analysis of fractions collected at the retention time of HPLC peak 1 (Fig. 2) which, when underivatized, gave two isomers

TABLE IV

HPLC–TSP-MS SPECTRA OF METHOXIMATED COMPOUNDS IN HPLC FRACTIONS CORRESPONDING TO PEAK 1 (1MO)

HPLC eluents: A = 0.1 *M* ammonium acetate buffer; B = 0.05 *M* ammonium acetate in methanol. HPLC gradient programme, 75–85% B in 20 min; flow-rate, 1 ml/min; interface, 95°C; vaporizer exit, 184°C; ion source, 300°C; filament on. Retention times in TSP are shown in parentheses. MO = Methoxyamine; Na = sodium ion. See also caption to Table I and Fig. 5 for fragment assignments.

[ASSIGN]$^+$	*m/z*	1MO1 (12.1)	1MO2 (14.3)	1MO3 (12.2)	1MO4 (14.8)	1MO5 (13.3)	1MO6 (13.9)
	106	–	–	–	–	3	5
	108	–	–	–	–	1	1
	120	–	–	–	–	–	2
	126	–	–	–	–	1	2
	130	–	–	–	–	1	6
	131	–	–	–	–	–	2
	135	–	–	–	–	–	2
X9 + H − H_2O	155	–	–	1	2	–	–
X9 + NH_4 − H_2O	172	–	–	2	2	–	2
X9 + H	173	–	–	3	3	–	–
Y10 + H	184	–	–	–	–	7	2
	187	–	–	–	–	–	4
X9 + NH_4	190	–	–	100	100	4	24
Y12 + H − H_2O	192	2	2	2	2	–	1
	195	–	–	4	1	–	–
X11 + NH_4 − H_2O	198	–	–	–	–	–	4
X11 + H	199	–	–	1	–	–	20
	200	1	–	1	–	–	5
Y10 + NH_4	201	–	–	5	1	100	35
	204	–	–	1	2	–	–
	206	–	–	–	–	3	1
Y12 + H	210	9	8	–	–	–	1
	214	–	–	–	–	–	3
	215	–	–	–	–	–	2
X11 + NH_4	216	–	–	6	–	–	100
	217	–	–	2	–	–	14
	221	–	–	–	–	–	2
Y12 + NH_4	227	100	100	4	2	4	6
	232	1	1	–	–	–	1
	234	–	–	–	–	–	1
	241	1	1	–	–	–	–
	279	–	–	–	–	2	–
M + H − H_2O − 32	292	1	–	1	3	2	5
M + NH_4 − H_2O − MO	294	1	1	–	1	1	3
M + H − 32	310	1	5	1	10	2	7
M + NH_4 − MO	312	1	8	1	11	2	4
M + H − H_2O	324	–	3	2	5	18	40
M + H	342	21	34	35	48	6	17
M + 15	356	–	–	–	–	–	4
M + Na	364	4	3	9	9	7	23

in TSP-MS (peaks 1a and b in Fig. 4), shows a total of six peaks labelled as 1MO1–1MO6 (see Table IV). Peaks 1MO1, 1MO2 and 1MO5, 1MO6 are present in the fractions collected across the upward and downward slopes of HPLC peak 1, respectively, whereas peaks 1MO3 and 1MO4 dominate in the centre portion of HPLC peak 1.

All of these signals (1MO1–1MO6) show an apparent molecular weight of 341 a.m.u., that is 29 a.m.u. over the apparent molecular weight of the original products (312 in Table I) and with an $[M+H]^+$ ion dominating over the corresponding ammonium adducts. Methoxime formation can therefore be inferred, proving the presence of a ketone or aldehyde group in the original compound. The two pairs of peaks, 1MO1–1MO2 and 1MO3–1MO4 can be correlated with the expected *syn-* and *anti-*isomers of the methoximes of peaks 1a and 1b (Fig. 4), respectively.

Fragmentation processes are important, as is shown by the base peaks at *m/z* 227 (1MO1–2), 190 (1MO3–4), 201 (1MO5) and 216 (1MO6). In the latter two cases mass spectral differences (Table IV) indicate that these peaks are not due to the methoxime *syn-* and *anti-*isomers but to different products. Their corresponding methoxime isomers can be found coeluting with 1MO3 by a detailed study of the ion chromatograms at *m/z* 201 and 216 (not shown in Table IV).

Fig. 5 shows the structures proposed for fragments X9 and Y12 in methoxime derivatives 1MO1–4 (see Table IV). The adduct ions $[Y12+NH_4]^+$ and $[X9+NH_4]^+$ correspond to the base peaks observed in the TSP-MS spectra of derivatives 1MO1–2 and 1MO3–4, respectively. Their abundance can be accounted for by fragmentation favoured by the hydroxyl group being in a position α to the methoxime. These base peaks are characteristics of the position of the α-ketol group within the fatty acid chain. Thus, these ions are useful diagnostic tools in the interpretation of these TSP-MS spectra. Accordingly, the ions in 1MO1–2 arise from the methoxime isomers of 13-hydroxy,12-keto octadecenoic acid (base peak at $[Y12+NH_4]^+$ in Table IV) whereas ions in 1MO3–4 arise from the isomers of 9-hydroxy,10-keto-octadecenoic

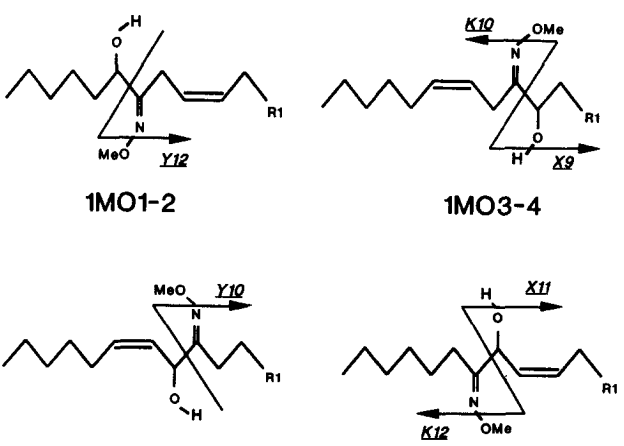

Fig. 5. Main fragmentation pathways observed in the spectra obtained by TSP-MS of methoxime derivatives 1MO1–6. R1 is $(CH_2)_6COOH$. Me = Methyl.

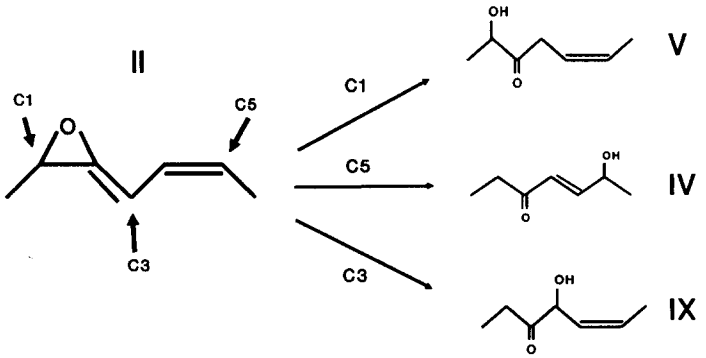

Fig. 6. Scheme illustrating the formation of metabolites IV and V (Fig. 1) through water attack on the C1 and C5 centre of the allene oxide precursor II. As attack on C3 leads to type IX structures detected in peak 1 of the HPLC profile of these incubates.

acid (base peak at $[X9+NH_4]^+$ in Table IV). The MO derivatives 1MO5 and 1MO6 show mass spectra similar to those of derivatives 1MO1–4 (Table IV), although their corresponding base peaks at m/z 201 and 216 do not correlate with fragments for the derivatives 1MO1–4. These ions have been assigned to the ammonium adducts of two fragments identified as Y10 and X11 in Fig. 5, respectively, and their structure is consistent with the MO derivatives of 11-hydroxy,10-keto (Y10) and 11-hydroxy,12-keto-octadecenoic (X11) acids. The addition of water on carbons 1 or 5 of the 1-oxo-2,4-pentadiene system in allene oxides IIa and IIb in Fig. 1 generates metabolites Va and Vb (peaks 1a, b in Fig. 4) as well as IVa and IVb (peaks 3a, b in Fig. 4) [10]. In contrast, the addition of water on carbon 3 (Fig. 6) of this common precursor would lead to the formation of the 11-OH,10-keto and 11-OH,12-keto metabolites (IXa,b in Fig. 7). Neither of these two metabolites were detected in the previous GC–MS study [3] and they have not been reported before in products arising from LOX activity on LA.

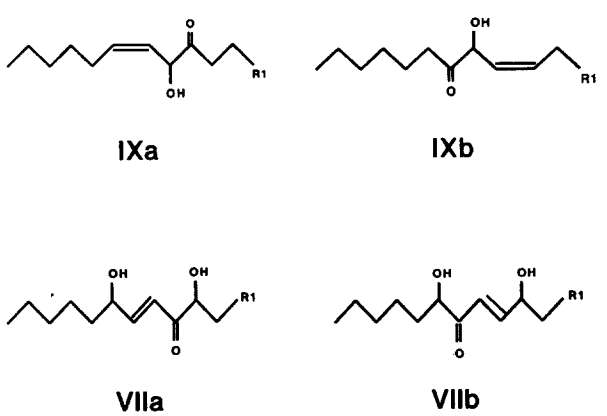

Fig. 7. Structures for the compounds found in HPLC peaks 1 (IXa and IXb) and 6 (VIIa and VIIb).

TABLE V

HPLC–TSP-MS SPECTRA OF METHOXIMATED COMPOUNDS IN HPLC FRACTIONS CORRESPONDING TO PEAK 3 (3MO)

HPLC eluents: A = 0.1 *M* ammonium acetate buffer; B = 0.05 *M* ammonium acetate in methanol. HPLC gradient programme, 75–85% B in 20 min; flow-rate, 1 ml/min; interface, 95°C; vaporizer exit, 184°C; ion source, 300°C; filament on. See also captions for Tables I and IV and Fig. 8 for fragment assignments.

[ASSIGN]$^+$	*m/z*	3MO1 (10.3)	3MO2 (12.0)	3MO3 (12.1)
	126	1	2	1
	130	1	–	1
S10+H	138	24	–	22
	140	1	–	1
Z10+NH_4	171	1	1	–
Y10+H	184	–	1	–
X9+NH_4	190	10	1	9
J11+H	199	2	–	2
Y10+NH_4	201	3	6	1
	202	1	2	–
X9+NH_4+14	204	1	–	2
	208	1	1	–
S12+H	210	3	4	–
J11+NH_4	216	7	–	6
	218	1	–	1
Z12+NH_4−H_2O	225	1	–	2
S12+NH_4	227	1	1	–
	236	–	2	–
Z12+NH_4	243	2	–	2
	290	3	3	2
M+H−H_2O−32	292	12	15	10
	293	6	5	3
M+NH_4−H_2O−MO	294	33	28	25
M+H−MO	295	10	10	11
M+NH_4−H_2O−MO+14	308	1	1	1
M+H−32	310	3	4	3
M+NH_4−MO	312	1	1	1
M+H−H_2O	324	17	100	21
M+H−2H	340	2	2	2
M+H	342	100	14	100
M+H+14	356	1	1	1
M+Na	364	12	11	7

Methoxime derivatives of fractions from peak 3

For the fractions corresponding to the elution time of HPLC peak 3 (Fig. 2), methoxime formation produces three distinct TSP-MS signals labelled 3MO1–3 in Table V and showing the mass spectral characteristics of the presence of a ketone group in the parent compound. The assigned molecular weight in this instance is also at 341 a.m.u., as expected from previous TSP data on the underivatized HPLC fraction (Fig. 4, compounds a, b). A detailed study of these spectra and of the selected ion chromatograms of major importance as diagnostic ions (*m/z* 190, 216, 225 and 243 for 3MO1 and 3MO3; *m/z* 201 and 210 for 3MO1 and 3MO2) indicates that the

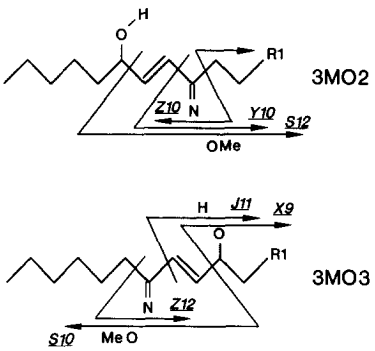

Fig. 8. Fragments observed in the spectra obtained by TSP-MS of derivatives 3MO2–3.

TSP-MS signal for 3MO1 is a mixture of derivatization isomers from components 3MO2 and 3MO3. Thus, as for HPLC peak 1, the two peaks arising from HPLC peak 3 fractions (peaks 3a and b in Fig. 4) produce four major peaks upon methoximation due to the respective methoxime *syn*- and *anti*-isomers of compounds IVa and IVb in Fig. 1.

The formation of ions arising from TSP-MS fragmentation is less favoured in this instance relative to the methoximes of α-ketol compounds. Nevertheless, the spectra of 3MO2 and 3MO3 can be differentiated by the presence of ions at m/z 201 and 210 ($[Y10+NH_4]^+$ and $[S12+H]^+$, respectively for 3MO2) and at m/z 138, 190,

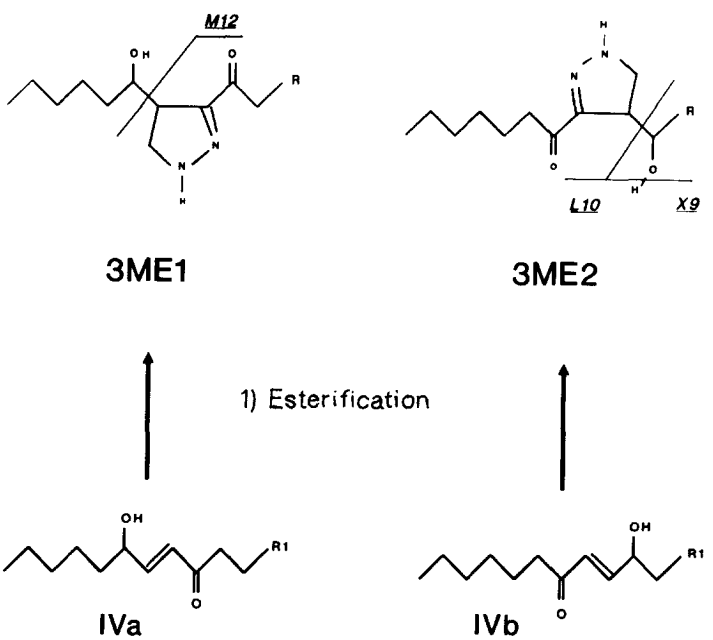

Fig. 9. Formation of diazomethane addition derivatives of compounds IVa and IVb upon methylation and fragments observed in their spectra obtained by TSP-MS.

216 and 243 ($[S10+H]^+$, $[X9+NH_4]^+$, $[J11+NH_4]^+$ and $[Z12+NH_4]^+$, respectively for 3MO3) (see Table V). These fragments are depicted schematically in Fig. 8.

It is interesting to note that in the course of a GC–MS study of the corresponding methyl ester–methoxime–trimethylsilyl ether (MEMOTMS) derivatives, the fractions collected from HPLC peak 3 showed a very peculiar behaviour which made attempts at MS identification difficult. In this instance, the resulting major GC peak shows a mass spectra with apparent molecular masses of 541 a.m.u., 114 a.m.u. higher than would correspond to the components of peak 1, even though, as indicated above, the TSP-MS spectra and HPLC retention characteristics suggest the presence of similar functional groups for HPLC peaks 1 and 3. However, the higher molecular mass could not be readily explained and, in addition, catalytic hydrogenation gave rise to two partially resolved peaks with an apparent molecular mass of 429 a.m.u. coincident with the corresponding hydrogenated derivatives of peak 1. Likewise, fully silylated and mixed methoxime–silyl derivatives produced electron impact mass spectra consistent with the structural features of hydroxy-keto octadecenoic acid type of compounds (IVa and IVb in Fig. 1).

The peculiar GC-MS mass spectra of MEMOTMS derivatives has been explained by the addition of a diazomethane molecule during the methylation reaction through 2+3 cyclo-addition of the diazomethane reagent to the activated double bond in the 4-hydroxy-2-alkenone system, as shown in Fig. 9 [3]. The addition of diazomethane to double bonds has been previously described for prostanoids [3,11,12]. The new chiral centre at C-10 or C-12 and/or the possible silylation of

TABLE VI

HPLC–TSP-MS SPECTRA OF METHYLATED COMPOUNDS IN HPLC FRACTIONS CORRESPONDING TO PEAK 3 (3ME)

HPLC eluents: A = 0.1 *M* ammonium acetate buffer; B = 0.05 *M* ammonium acetate in methanol. HPLC gradient programme, 70–85% B in 15 min; flow-rate, 1 ml/min; interface, 95°C; vaporizer exit, 186°C; ion source, 300°C. See also captions for Tables I and IV and Fig. 9 for fragment assignments.

$[ASSIGN]^+$	*m/z*	3ME1 (15.4)	3ME2 (16.1)
	151	1	–
L10+H−28	153	1	–
L10+H	181	4	5
L10+H+2	183	1	–
$L10+NH_4$	198	3	4
$X9+NH_4$	204	8	9
	237	1	–
M12+H−28	239	2	1
M12+H	267	4	6
$M12+NH_4$	284	1	1
$M+H-H_2O-28$	323	1	1
	324	1	1
M+H−28	341	1	–
$M+H-H_2O-2H$	349	1	2
M+H	369	100	100
M+Na	391	20	11

isomers explains the isomers found for this structure. In contrast, if the order of sequential derivatization is changed so that methoximation is carried out before methylation, no such addition is observed.

TABLE VII

HPLC–TSP-MS SPECTRA OF METHOXIMATED COMPOUNDS IN HPLC FRACTIONS CORRESPONDING TO PEAK 6 (6MO)

HPLC eluents: A = 0.1 *M* ammonium acetate buffer; B = 0.05 *M* ammonium acetate in methanol. HPLC gradient programme, 60–85% B in 25 min; flow-rate, 1 ml/min; interface, 95°C; vaporizer exit, 190°C; ion source, 300 °C; filament on. Fragments in parentheses indicate alternative structures for the observed ion. See also captions for Tables I and IV and Fig. 10 for fragment assignments.

[ASSIGN]$^+$	*m/z*	6MO1 (14.8)	6MO2 (15.2)	6MO3 (15.8)
	102	2	–	3
	104	–	1	9
	112	3	1	2
Z(R)10 + H − H_2O	136	–	2	–
	146	–	–	3
	152	9	–	8
R(Z)10 + H	154	7	2	8
X9 + NH_4 − H_2O	155	2	–	3
	156	6	–	3
Z(R)10 + NH_4	171	9	5	4
X9 + NH_4 − H_2O	172	3	2	2
X9 + H_4	173	3	3	–
X9 + NH_4	190	97	100	39
	192	3	2	1
	195	2	4	–
J11 + NH_4 − H_2O	198	–	–	4
J11 + H	199	7	–	18
T10 + H	200	1	–	3
	202	1	–	2
	204	16	2	41
Z(R)12 + H − H_2O	208	1	–	3
J11 + NH_4	216	38	4	93
T10 + NH_4	217	5	1	12
	221	–	–	6
Z(R)12 + NH_4 − H_2O	225	7	–	22
Z(R)12 + H	226	3	–	8
	241	–	–	2
Z(R)12 + NH_4	243	47	4	100
	248	2	–	5
	257	1	–	1
	290	1	1	2
	292	3	2	4
M + H − H_2O − 32	308	4	3	6
M + NH_4 − MO − H_2O	310	11	4	11
	311	2	1	2
	322	1	1	21
M + H − H_2O	340	11	33	87
M + H	358	100	8	76
M + Na	380	35	10	54
	396	3	–	5

TSP-MS analysis of the methylated fraction from peak 3

The TSP-MS analysis of methyl derivatives of the fractions obtained from peak 3 provides additional information about the formation of an dihydropyrazole ring by diazomethane addition, as postulated in the preceding section. The TSP chromatogram shows two major signals with very similar spectra. According to these data, the molecular mass of both components is 368 or 56 a.m.u. greater than that of the free compounds and 42 a.m.u. greater than in the expected methyl ester derivative (Table VI) which is indicative of diazomethane addition (42 a.m.u.).

Some useful fragmentation can also be observed. Diagnostic fragments are labelled L10 (at *m/z* 181 and 198, $[L10+H]^+$ and $[L10+NH_4]^+$, respectively), M12 (at *m/z* 267 and 284, $[M12+H]^+$ and $[M12+NH_4]^+$, respectively) and X9 (at *m/z* 204, $[X9+NH_4]^+$ (see Fig. 9). Thus the TSP-MS analysis of the methyl derivative facilitates the determination of the positions of the double bond and the hydroxyl and ketone groups. Fragments L10, X9 and M12 are characteristic of the 9 hydroxy- and 13-hydroxy-isomers, respectively.

An interesting ion which would be difficult to account for by solvent addition and/or water elimination is that observed at *m/z* 349 (Table IV). This ion could arise from a diazomethane loss from the $[M+Na]^+$ ion. However, ions due to Na^+ addition do not usually show signals from elimination or fragmentation processes [13] and furthermore, ions due to diazomethane loss from $[M+H]^+$ were not detected in this instance. Accordingly, the formation of this ion could be explained by the loss of a hydride ion involving redox processes. The same considerations apply to ions L10 and M12 with apparent molecular masses of 180 and 266 a.m.u., respectively. The formation of a highly stable aromatic pyrazole ring structure could be the factor behind the favoured loss of hydride ions in this spectra. Other ions in Table IV involving losses of 28 a.m.u. could be ascribed to the loss of an N_2 moiety.

Methoxime derivatives of fractions from peak 6

The TSP-MS analysis of the methoximated compounds in the HPLC eluate fraction collected at the retention time of peak 6 (Fig. 1) shows a group of three signals only partially resolved and labelled 6MO1–3 in Table VII. All of these ions show an apparent molecular weight of 357 a.m.u., also 29 a.m.u. over the apparent molecular weight of the underivatized peak 6 and indicative of a ketone moiety. The selected ion traces from *m/z* 190, 216 and 243 suggest the presence of at least four distinct products in this fraction. As for the HPLC peak 3 described in the preceding section, the TSP-MS spectrum for 6MO1 corresponds to a mixture of isomers from 6MO2 and 6MO3, whereas the latter can be characterized by their dominant ions at *m/z* 190 and at *m/z* 216 and 243, respectively. Thus, it seems that in this instance *syn*- and *anti*-isomers of the methoximes are present from two positional isomers.

The assignments of the TSP-MS fragments observed for the 6MO derivatives are illustrated in Fig. 10, corresponding to the methoximes of the 9,13-dihydroxy-10-keto,11-octadecenoic acid and the 9,13-dihydroxy-12-keto,10-octadecenoic acid (illustrated as 6MO2 and 6MO3, respectively, and as VIIa and VIIb in Fig. 5). These fragmentations are analogous to those observed for the 1MO1 and 3MO derivatives. As in these instances, the hydroxyl group α to the oxime moiety directs the ion profile. Thus, fragment Y12 in the 1MO1 and 1MO2 derivatives (Fig. 5) gives rise to fragment Z12 in 6MO3 (Fig. 10). This fragment is found at 16 a.m.u. higher because of the

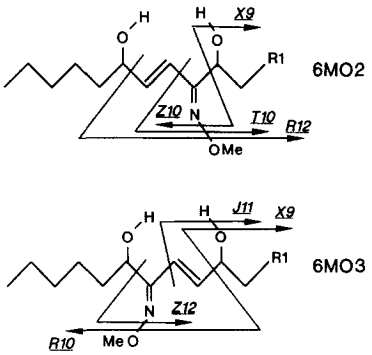

Fig. 10. Fragments observed in the spectra of derivatives 6MO2 and 6MO3 obtained by TSP-MS.

presence of an additional hydroxyl group and shows the expected adducts generated by the loss of water. The ions derived from fragments R12 and Z10 from 6MO2 are isobaric with the ions derived from fragments Z12 and R10 in 6MO3. Ions Z10 and Z12 are produced by fragmentations equivalent to those observed for the 1MO derivatives and thus are favoured relative to R10 and R12 (Table VII). However, the ion abundances for R10 and Z10 derived fragments in 6MO2 and 6MO3 do not distinguish between the two compounds. In all of the methoxime derivatives discussed in this paper, those adducts containing the carboxylic acid group are more abundant than the equivalent fragments containing the end part of the molecule. This indicates that ionization is driven by the carboxyl moiety and can be related to the low abundance of equivalent adduct fragments in the case of derivatized thromboxane [8]. Thus, fragment Z12 containing the carboxyl moiety is favoured relative to its isobare R12 and in this instance the relative abundance of the corresponding ions is important and allows for a differentiation between derivatives 6MO2 and 6MO3.

Finally, fragmentation at J11 gives very prominent ions in 6MO3 (m/z 216, RA 93% as shown in Table VII). This ion shows the same m/z ratio as the corresponding adduct arising from fragmentation X11 in 1MO6 (Table IV) and indicates the presence of a 11,12-ketol system. Nevertheless, the GC–MS data do not justify such an structure. Likewise, the ion at m/z 216 appears at a lower abundance in the TSP-MS spectrum of 3MO3 (Table V), together with the ion at m/z 243 corresponding in both instances to the fragment Z12 (Tables V and VII). The relative abundances of these two ions in both derivatives supports the formation of J11 from Z12 by nitrile elimination.

Methoxime derivatives of fractions from peak 7

The same approach applied to the eluate fractions from HPLC peak 7 (Fig. 2) did not result in any changes in the TSP-MS spectra, so that no ketone or aldehyde groups should be expected in its structure.

In summary, the information provided at this point by TSP indicates that the compounds present in the HPLC fractions collected from peaks 1 and 3 (Fig. 3) are positional isomers of hydroxy-keto-octadecenoic acids. The differences in the extent of fragmentation of components 1MO and 3MO could be ascribed to the different position of the hydroxyl and methoxime groups relative to the double bound.

Along these lines, an α-ketol type of structure justifies the extensive fragmentation observed on TSP-MS as well as the adduct ions observed for the compounds derived from HPLC peak 1. These fragments ions allow the assignment of the position of hydroxy and keto groups in the molecule and characterize the compounds found in fractions collected from HPLC peak 1 as the 9-hydroxy,10-keto-, 13-hydroxy,12-keto-, 11-hydroxy,10-keto- and 11-hydroxy,12-keto-octadecenoic acids and compounds in HPLC fractions from peak 3 as the 9-hydroxy,12-keto- and 13-hydroxy,10-keto-octadecenoic acid. The double bond position in these compounds cannot be determined from the TSP-MS data alone. However, fragments from the methoximes of peak 3 indicate that the double bond is in positions 10 (9-hydroxy,12-keto) and 11 (13-hydroxy,10-keto).

The derivative products from HPLC peak 6 could be ascribed to metabolites with the structural features of dihydroxyketo octadecenoic acids. Fragmentations, which are equivalent to those in the methoximes from peaks 1 and 3, indicate that at least one hydroxyl group is in a position α to the oxime. The second hydroxyl moiety and the double bond are possibly placed in positions which, relative to the oxime, are identical to those in the methoximes of peak 3. Overall, the observed TSP-MS fragments ions allow the identification of these compounds as 9,13-dihydroxy,10-keto, 11-octadecenoic and 9,13-dihydroxy,12-keto,10-octadecenoic acids (see VIIa and VIIb in Fig. 7).

Compounds in the HPLC fractions corresponding to peak 7 can be identified as trihydroxyoctadecenoic (or dihydroxyepoxyoctadecanoic) acids. However, the positions of the hydroxyl groups and double bonds cannot be pinpointed from the TSP-MS data alone. The necessary additional information leading to further identification of the structural features of these compounds was obtained from a parallel GC–MS study of the corresponding fractions, as reported elsewhere [3]. The GC–MS data allowed the identification of two positional trihydroxyoctadecenoic acid isomers with the structures of compounds VIa and VIb in Fig. 1.

CONCLUSIONS

Despite the supposedly greater amount of information that can be obtained by GC–MS techniques. HPLC–TSP-MS can provide molecular information much more rapidly which can be of critical importance for structural identification when giving rise to unexpected derivatization products, as shown for the metabolites IV and VII.

Positive and negative TSP-MS give additional information on the minimum number of groups which can lose water molecules and on the possible presence of conjugated systems in the intact molecular or in the dehydration products. It is also noteworthy that in an application such as that reported here, in which the precursor compound is known (LA) and where the number of double bonds due to oxo or acid groups can be determined through the analysis of methylated or methoxime derivatives, the TSP-MS information gives by itself a reliable approximation to the atomic composition and functional groups of the compound of interest.

Through the use of derivatization reactions is is possible to obtain products which are liable to undergo fragmentation reactions due to thermal degradation, ionization or collision processes in the ion source. Regardless of their mechanism of formation, these fragmentations provide a degree of structural information which, as

shown here, leads to easier interpretations and the same conclusions as obtained by the more elaborate GC–MS analyses.

This HPLC–TSP-MS assay has facilitated the detection of two new structures (IXa and IXb in Fig. 7) derived from LOX activity in maize embryos which were difficult to characterize by standard GC–MS techniques. The structure of the new metabolite VII, and those of metabolites IV and V, can be also readily established from the TSP-MS data for the free and oximated compounds.

ACKNOWLEDGEMENTS

This work was supported in part by grants 89/0386 from FIS and BIO88:0162 from CICYT (Spain).

REFERENCES

1 V. A. Vick and D. C. Zimmerman, in P. K. Stumpf and E. E. Conn (Editors), *The Biochemistry of Plants*, Vol. 9, Academic Press, London, 1987, pp. 53-90.
2 D. F. Hildebrand, *Physiol. Plant.*, 76 (1989) 249.
3 J. Abián, E. Gelpí and M. Pagès, *Plant Physiol.*, 95 (1991) 1277.
4 M. J. Davies and T. A. Mansfield, in F. T. Addicott (Editor), *Abscisic Acid*, Praeger, New York, 1983, pp. 237-268.
5 M. Pla, A. Goday, J. Vilardell, J. Gomez and M. Pagès, *Plant Mol. Biol.*, 13 (1989) 385.
6 A. Goday, D. Sanchez Martinez, J. Gomez, P. Puigdomenech and M. Pagès, *Plant Physiol.*, 88 (1988) 564.
7 J. Abián, J. Oriol Bulbena and E. Gelpí, *Biomed. Environ. Mass Spectrom.*, 16 (1988) 215.
8 J. Abián and E. Gelpí, *J. Chromatogr.*, 562 (1991) 153.
9 J. Abián and E. Gelpí, presented at the *39th ASMS Conference, Nashville, TN, May 19–24, 1991.*
10 M. Hamberg, *Biochim. Biophys. Acta*, 920 (1987) 76.
11 A. F. Cockerill, N. J. A. Gutteridge, D. N. B. Mallen, D. J. Osborne and D. M. Rackham, *Biomed. Mass Spectrom.*, 4 (1977) 187.
12 A. F. Cockerill, *Prostaglandins*, 13 (1966) 1036.
13 J. A. Yergey, H.-Y. Kim and N. Salem Jr., *Anal. Chem.*, 58 (1986) 1344.